Application and Development of Synthetic Polymer Membranes. II. Separation of Aqueous Ethanol Solution Through Poly(*tert*-Butyl Methacrylate-Co-Styrene) Membranes

MASAKAZU YOSHIKAWA*, TOMOKI OHSAWA, MASATAKA TANIGAKI, AND WATARU EGUCHI,
Department of Chemical Engineering, Faculty of Engineering, Kyoto University, Kyoto 606, Japan

Synopsis

Separation of aqueous ethanol solution was carried out by pervaporation using a membrane which consisted of common polymer membranes. A membrane obtained from poly(*tert*-butyl methacrylate-co-styrene) was effective for a selective separation of ethanol from aqueous ethanol solution by pervaporation technique. The pervaporation of ethanol–water mixture through the present membranes was analyzed as a solution–diffusion process, on the assumption that the both diffusion coefficients of each component are an exponential function of ethanol concentration.

INTRODUCTION

The problem of the inevitable exhaustion of our fossil fuels is one of the most serious challenges we will have to face. There exist two ways to meet this problem: One is to use biomass energy,[1-4] which is a clean and regenerative energy source; the other is solar energy,[5-9] which is also clean and inexhaustible. Because ethanol, one of the biomass energy sources to be tapped, is not only an energy resource but also a chemical raw material in its own right,[10] its production will soon be an important industry in itself.

There are a couple of ways, by using membranes, to separate the aqueous ethanol solution from its raw material. One is the selective removal of water through use of special membranes;[11] the other is to use membrances that preferentially allow ethanol to permeate through.[12-25]

To accomplish this selective separation of ethanol by pervaporation, it is necessary to develop novel polymers from common monomers to serve as the material of the special membranes. One of the authors of this article has found such a polymer—poly(methyl methacrylate-co-styrene)[24]—that has the potential to be used as an ethanol permeable membrane by using the membrane polarity value[26,27] as the index to design the molecular structure of membrane materials for the separation of aqueous ethanol solution.

*To whom all correspondence should be addressed.

Journal of Applied Polymer Science, Vol. 37, 299–315 (1989)

CCC 0021-8995/89/020299-17$04.00

On the basis of this idea, we prepared poly(*tert*-butyl methacrylate-co-styrene) membranes, and investigated the selective separation of aqueous ethanol solution through the present membranes. Preliminary experiments show that these membranes might also possibly be applicable to selective separation of ethanol from water–ethanol mixture.[25] The present article deals with pervaporation of water–ethanol mixtures through poly(*tert*-butyl methacrylate-co-styrene) membranes.

EXPERIMENTAL

Materials

Tert-Butyl methacrylate (**1**), styrene (**2**), and 2,2′-azobis(2-methylpropionitrile) (AIBN) were purified by the usual methods. Toluene was used without further purification. Deionized water was used.

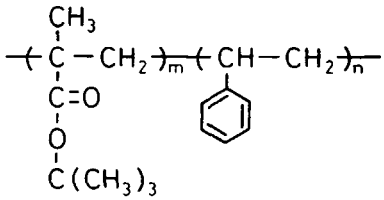

Code	m	n
T1	0.023	0.977
T2	0.049	0.951
T3	0.092	0.908
T4	0.142	0.858

Poly(*tert*-butyl methacrylate-co-styrene)s (T1–T4) were prepared as follows: Compounds **1** and **2** were placed in an ampule with AIBN and sealed in a nitrogen atmosphere. The copolymerization was carried out at 45°C for 4 days with shaking. The results are summarized in Table I.

Preparation of Membranes

All membranes were obtained by casting from toluene solution (65 g dm^{-3}). The solutions were poured onto glass plates with applicators (casting thickness, 0.254 mm), and the solvent was allowed to evaporate at ~ 40°C for 3 h. Thickness of the membrane was approximately 10 μm.

Pervaporation

The apparatus used to obtain pervaporation data is illustrated in Figure 1, and the cross section of the liquid permeation cell (8 in Fig. 1) is given in Figure 2. The whole apparatus was made of glass. The upstream compartment

TABLE I
Results of Copolymerization[a]

Polymer	Monomer 1 (g)	Monomer 2 (g)	AIBN (mg)	Time (days)	Yield (g)	Mol fraction of 1 in Monomer	Mol fraction of 1 in Polymer	η_{sp}/C[b] ($dm^3\ g^{-1}$)
T1	0.858	30.62	246	4	27.00	0.020	0.023	0.165
T2	2.138	29.68	243	4	26.45	0.050	0.049	0.191
T3	4.269	28.12	247	4	27.74	0.100	0.092	0.162
T4	6.394	26.56	246	4	27.33	0.150	0.142	0.138

[a] Polymerization temperature, 45°C.
[b] Reduced viscosity was measured at $C = 1.0\ g\ dm^{-3}$ toluene at 25°C.

had a capacity of ~ 175 cm^3, and the membrane area in contact with liquid was 10.5 cm^2. The liquid permeation cell was thermostatted at 15°C by a water jacket. As shown in Figure 1, the liquid permeation cell (8) was connected to an oil rotary pump (1) so that the downstream pressure was maintained: 400 Pa (3.0 torr) or 3330 Pa (25.0 torr). The pressure was measured with an oil manometer (3). After the membrane was mounted in the liquid permeation cell, the feed liquid was supplied to the cell and allowed to stand overnight. The stirring was about 200 rpm. The trap for condensing permeate (4) or (5) was cooled using liquid nitrogen after the downstream side had been evacuated. During the course of pervaporation experiments, the trap for condensing permeate (4) or (5) was switched at appropriate time intervals. The flux was obtained by weighing the trapped permeate. The separation factor α was calculated by determining the composition of the feed liquid mixtures and the permeates. The composition analysis was carried out on a Shimadzu/ GC-8A gas chromatograph with a 3.1-m-long column packed with polyethylene glycol 6000 on Shimalite TPA.

$$\alpha = \frac{Y_{ethanol}/Y_{water}}{X_{ethanol}/X_{water}} \tag{1}$$

where the Y_i are the weight fractions of permeates and the X_i those of feeds, respectively.

Determination of Membrane Polarity Value

Membrane polarity value in terms of Dimroth's solvent polarity value [E_T(25°C)] of membranes were measured as described previously, using 1-octadecyl-3, 3-dimethyl-6′-nitrospiro(indoline-2, 2′-2H-benzopyran) as the indicator.[26] A 500 W xenon lamp was used as the light source. The membrane was illuminated with UV light using a Corning color filter no. 7-54. Absorption spectra were measured with a Shimadzu MPS-2000 multipurpose recording spectrophotometer.

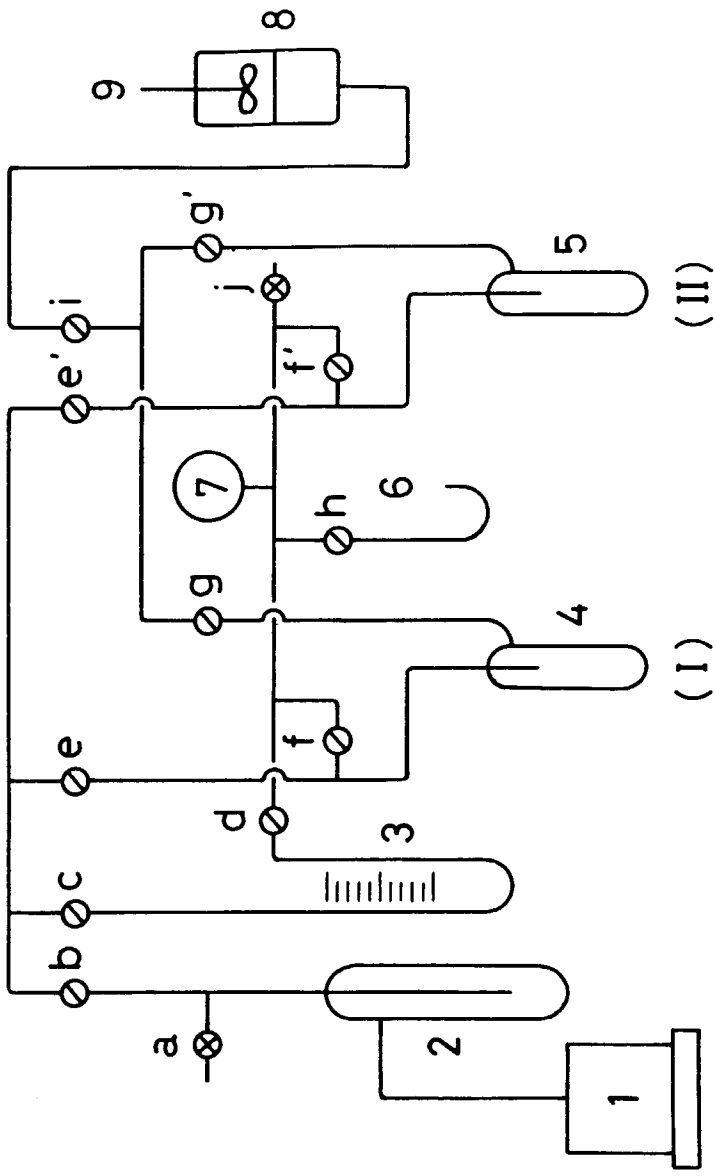

Fig. 1. Schematic diagram of apparatus for pervaporation studies: (1) oil rotary pump; (2) trap for safety; (3) oil manometer [maximal pressure, 4017 Pa (30.0 torr)]; (4, 5) trap for condensing permeates; (6) mercury manometer [maximal pressure, 1.071×10^5 Pa (800 torr)]; (7) gas holder ($\sim$ 1 dm^3); (8) liquid permeation cell; (9) stirrer.

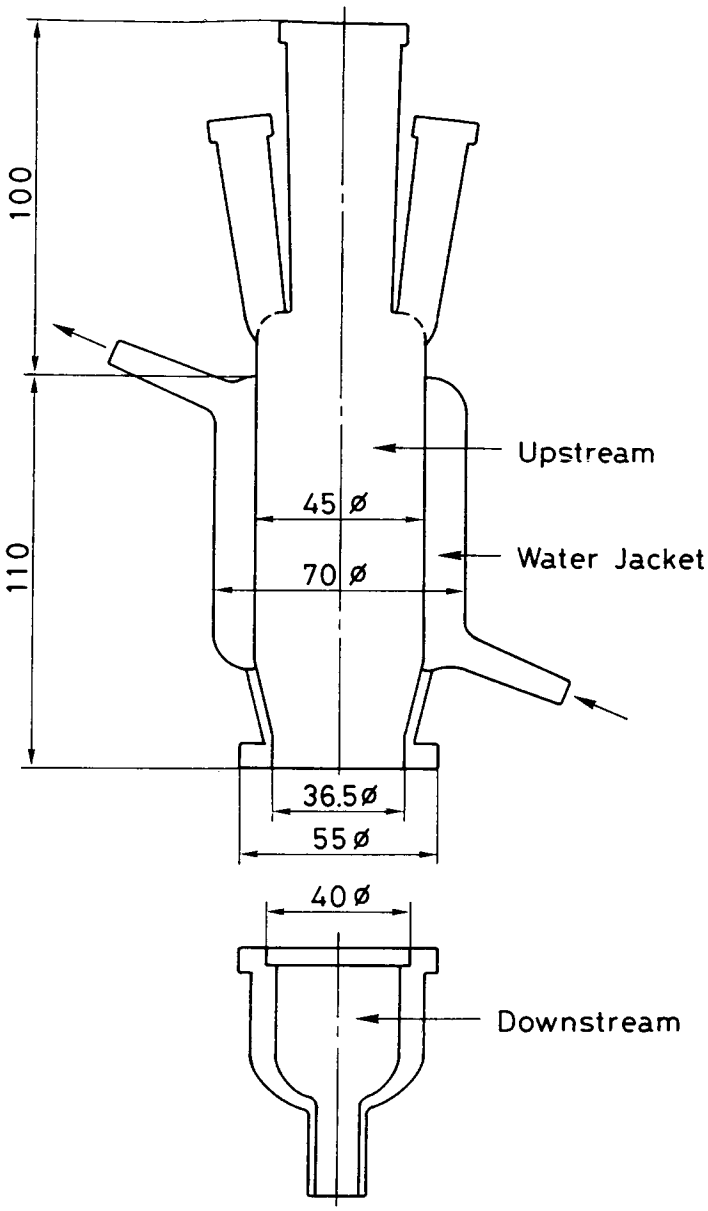

Fig. 2. Liquid permeation cell.

Measurement of Degree of Swelling

A piece of membrane after drying to constant weight (W_d) was immersed in ethanol or water at 15°C. When the sorption equilibrium was reached, the piece was weighed rapidly after blotting free surface liquid. The degree of swelling for membranes was defined by

$$\text{degree of swelling} = \frac{W_s - W_d}{W_d} \times 100 \tag{2}$$

where W_d and W_s denote the weight of dry and solvent swollen membrane, respectively.

Estimation of Solubility Parameter

The solubility parameter (δ_{sp}), which is made up of dispersion forces (δ_d), dipole forces (δ_p), and hydrogen bonding (δ_h), were calculated for each membrane, as in references[28-30]. The space distance between ethanol and membrane (DEM) and that between water and membrane (DWM) are defined by eqs. (3) and (4) with the following values: $\delta_{d,E} = 7.73$ cal$^{1/2}$ cm$^{-3/2}$, $\delta_{p,E} = 4.3$ cal$^{1/2}$ cm$^{-3/2}$, and $\delta_{h,E} = 9.5$ cal$^{1/2}$ cm$^{-3/2}$ for ethanol[29]; and $\delta_{d,W} = 9.54$ cal$^{1/2}$ cm$^{-3/2}$, $\delta_{p,W} = 8.72$ cal$^{1/2}$ cm$^{-3/2}$, and $\delta_{h,W} = 8.62$ cal$^{1/2}$ cm$^{-3/2}$ for water[31]. The equations themselves are:

$$\mathrm{DEM} = \left[(\delta_d - \delta_{d,\mathrm{E}})^2 + (\delta_p - \delta_{p,\mathrm{E}})^2 + (\delta_h - \delta_{h,\mathrm{E}})^2\right]^{1/2} \tag{3}$$

$$\mathrm{DWM} = \left[(\delta_d - \delta_{d,\mathrm{W}})^2 + (\delta_p - \delta_{p,\mathrm{W}})^2 + (\delta_h - \delta_{h,\mathrm{W}})^2\right]^{1/2} \tag{4}$$

RESULTS AND DISCUSSION

Characterization of Membranes

Membrane polarity values E_T(25°C), together with wavelength of the absorption maximum of the indicator, degrees of swelling for ethanol and water, DEM and DWM are summarized in Table II.

Membrane polarity values for these membranes increased with the increase in the tert-butyl methacrylate (1) content in the membrane as observed in poly(methyl methacrylate-co-styrene) membranes.[24]

From the data on degree of swelling, these four membranes showed a tendency to swell with ethanol, while swelling only a little with water. The degree of swelling with ethanol increased with the increase in 1 content, and this tendency correlated with the decrease of DEM. As for DWM, such correlation was not observed. This is due to the fact that the distance between the solubility parameter of membrane and that of water is too far for water to swell the membrane.

TABLE II
Characterization of Membranes

Membrane	λ_{max}^{Vis} (nm)	E_T(25°C) (kcal mol^{-1})	Degree of swelling (%)		DEM[a] (cal$^{1/2}$ cm$^{-3/2}$)	DWM[a] (cal$^{1/2}$ cm$^{-3/2}$)
			In ethano	In water		
T1	609	29.5	4	1	9.7	11.5
T2	607	30.2	5	1	9.4	11.3
T3	607	30.2	9	1	9.1	11.1
T4	605	31.0	12	2	8.9	10.9

[a] 1 cal$^{1/2}$ cm$^{-3/2}$ = 2.046 J$^{1/2}$ cm$^{-3/2}$.

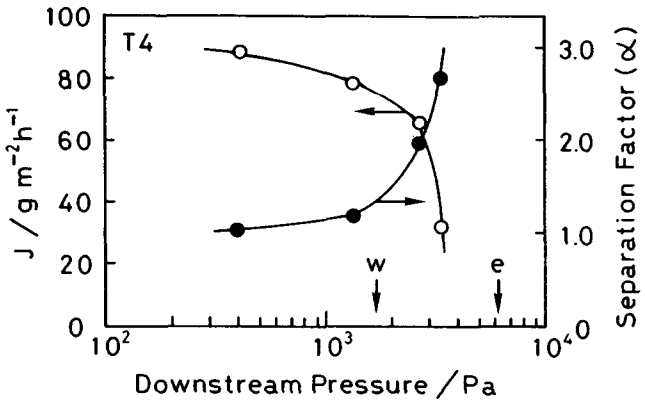

Fig. 3. Effect of downstream pressure on separation of aqueous ethanol solution through membrane T4 at 15°C. (Weight fraction of ethanol in feed, 0.502.)

Dependence of Operating (Downstream) Pressure

Figure 3 shows the dependence of membrane performance on downstream pressure. The flux and separation factor for T4 membrane are plotted at various downstream pressures for a fixed feed concentration of 0.502 weight fraction ethanol. These data indicate that there is a tendency for flux to decrease as downstream pressure is increased, while separation factor increases with the increment of operating pressure. Vapor pressures for ethanol and water at the operating temperature of 15°C are ~ 4399 Pa (33.0 torr)[32] and 1706 Pa (12.8 torr),[32] respectively. For downstream pressure greater than 1706 Pa, both the decrease in flux and the increase of separation factor will be observed prominently. In the present case, an increase in downstream pressure increases the concentration of the more volatile component, in the present case, ethanol in the permeate as reported in the pervaporation of hexane–heptane mixture through polyethylene film by Greenlaw et al.[33]

The remainder of this paper, then, is devoted to the description of our work with the downstream pressure of both 400 Pa (3.0 torr) and 3330 Pa (25.0 torr).

Dependence of Feed Composition

Figure 4 shows results of the pervaporation experiments for membranes T1–T4, where the weight fraction of ethanol in permeate are plotted as a function of ethanol fraction in feed. Figures 5 and 6 give the separation factor (α) and the total fluxes plotted against the weight fraction of ethanol in feed. From Figure 4, under the operating pressure of 3330 Pa, these four kinds of membranes preferentially permeated ethanol in the wide feed fraction range except in the high ethanol feed fraction region, where the weight fraction of ethanol in feed was more than around 0.88. Under the operating pressure of 400 Pa, at the region where the weight fractions in feeds were low, ethanol was preferentially permeated, as reported in the pervaporation of ethanol–water mixtures through poly(acrylic acid-co-styrene) membrane,[21] contrary to the results obtained under the operating pressure of 3330 Pa.

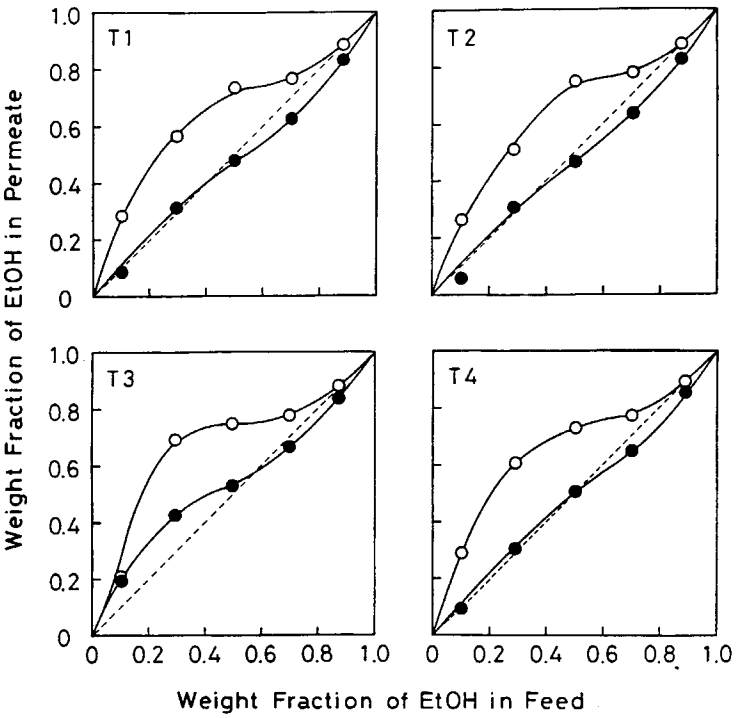

Fig. 4. Effect of feed composition on the separation of aqueous ethanol solution through poly(*tert*-butyl methacrylate-co-styrene) membranes. Operating temp, 15°C; downstream pressure: (●) 400 Pa (3.0 torr); (○) 3330 Pa (25.0 torr).

As for dependence of separation factor on feed composition, separation factor α tended to decrease with the increase in ethanol feed fraction except in the low ethanol fraction region, where the weight fraction of ethanol in feed was less than around 0.3. The separation factor toward ethanol ranged from 0.5 to 2.1 under the operating pressure of 400 Pa and from unity to 5.3 under that of 3330 Pa, even though the present membranes were merely prepared from common polymers such as methacrylic ester–styrene copolymers.

The total flux values for each membrane increased exponentially with the increase in ethanol feed fraction as was expected from the fact that the present membranes preferentially permeated ethanol.

As mentioned above, common polymer membranes from copolymers of methacrylic ester and styrene preferentially permeated ethanol from aqueous ethanol solution like acrylic acid–styrene[21] or methyl methacrylate–styrene[24] copolymer membrane. Further studies such as combination of methacrylic esters and styrene, control of membrane morphology by membrane preparation process, operating conditions, and so forth, may open the door to utilization of such common polymers as membrane materials for separation of ethanol from aqueous ethanol solution.

Permeation Mechanism

To study the permeation mechanism of ethanol and water through present membranes, we separated the observed fluxes under the downstream pressure of 400 Pa into their respective ethanol and water fluxes, so that they can be

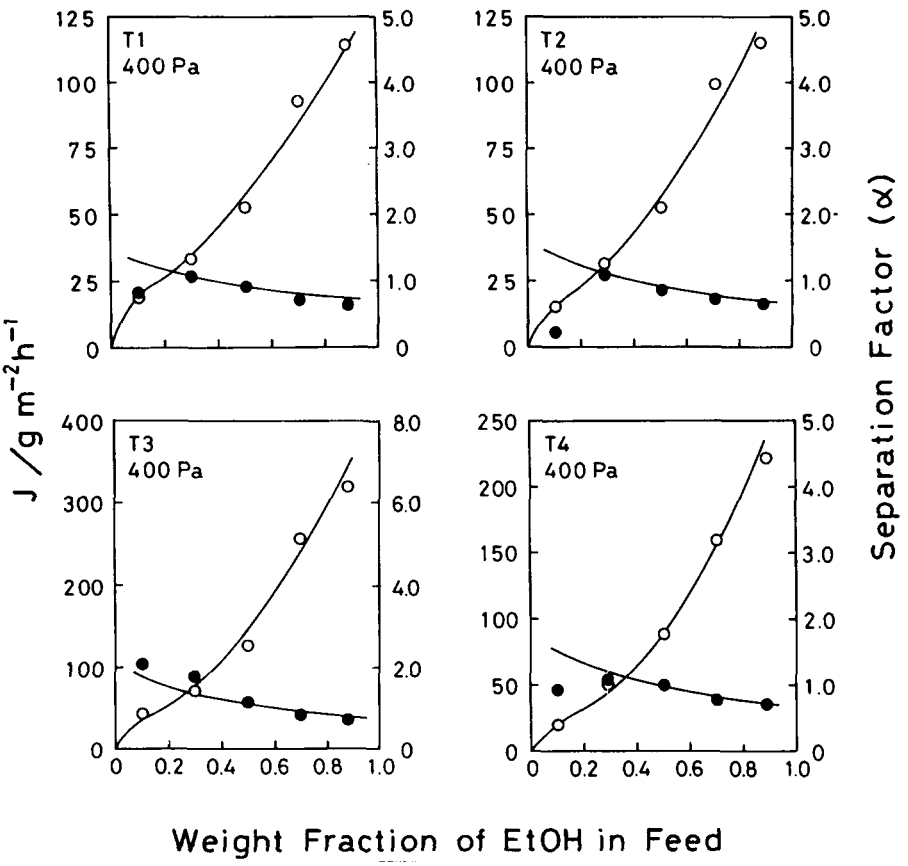

Fig. 5. Effect of feed composition on separation factor (α) and total flux in ethanol–water pervaporation through membrane Ts. Operating temp, 15°C; downstream pressure, 400 Pa (25.0 torr); (●) separation factor; (○) total flux; (——) calculated, according to eqs. (10), (16), and (18), and taking the values for coefficients summarized in Table III.

plotted against its feed concentration as previously reported.[11,21,24,34-38] The reason why we studied the permeation mechanism under the operating pressure of 400 Pa is as follows: Under the downstream pressure of 400 Pa, it is possible to assume, as most do, that the permeant concentration at the downstream side of the membrane is zero. In this situation, we could derive the permeation equation by thinking about only the permeation of substance in the membrane. As an example of the relationship between each component-flux and feed concentration, those for membrane T4 under the operating pressure of 400 Pa is shown in Figure 7. The curve of ethanol showed an exponential profile. On the other hand, water flux dependence on its feed concentration was more complicated having maximum flux value. Other relationships between component-flux and feed concentration of membranes T1, T2, and T3 under the operating pressure of 400 Pa gave similar profiles as shown in Figure 7.

For permeation of ethanol through present membranes, the diffusion coefficient D usually depends on the local concentration of ethanol.[39-46] In some cases the concentration dependence of the diffusion coefficient has been

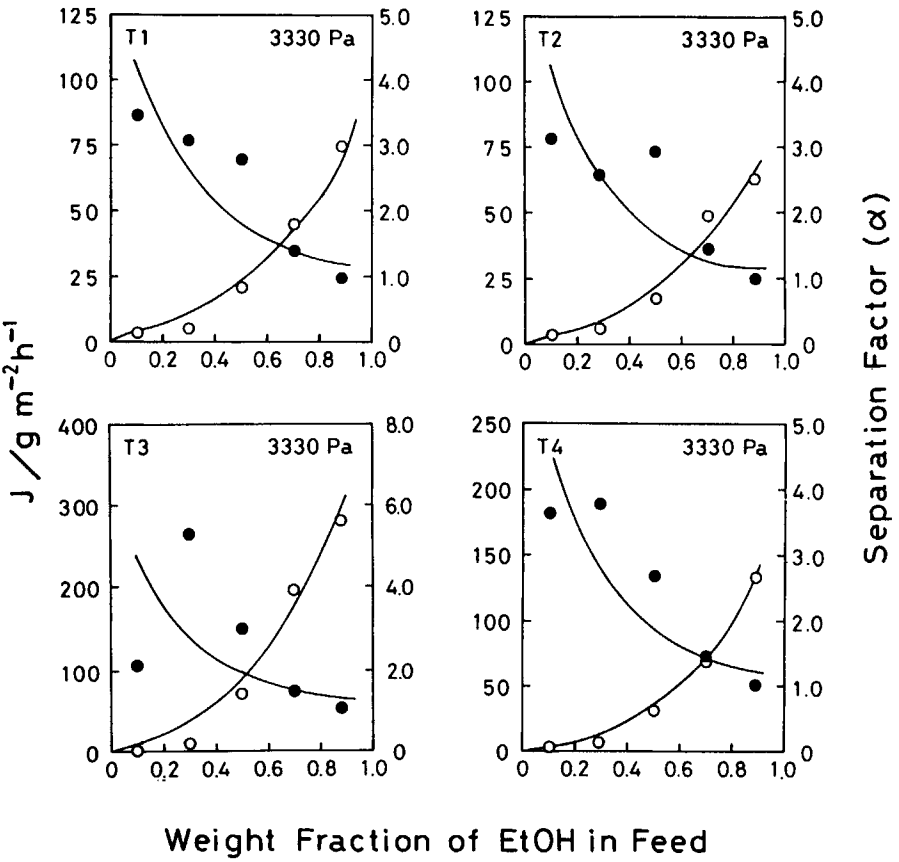

Fig. 6. Effect of feed composition on separation factor (α) and total flux in ethanol–water pervaporation through membranes Ts. Operating temp, 15°C; downstream pressure, 3330 Pa (25.0 torr; (●) separation factor; (○) total flux.

reported to be linear,

$$D = D_0(1 + a\bar{C}) \tag{5}$$

and in the others it was observed to have an exponential form,

$$D = D_0 \exp(b\bar{C}) \tag{6}$$

In these two equations, D_0 is the D value in the limit of zero permeant concentration; a and b are coefficients characteristic of the membrane/permeant interaction; $\bar{C}$ denotes the permeant concentration in the membrane. Equation (6) will be used here, since it is more suitable in cases where the diffusion coefficient more strongly depends on concentration. For ethanol permeation through these membranes, eq. (6) becomes

$$D_E = D_{0,E} \exp(b_{EE}\bar{C}_E) \tag{7}$$

From eq. (7) and the Fick's first law of diffusion, ethanol flux through the

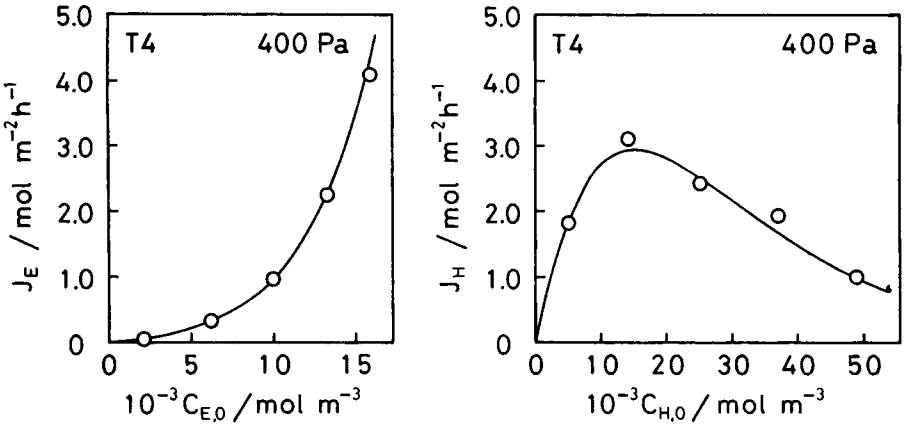

Fig. 7. Effect of ethanol and water concentrations on their fluxes in ethanol–water pervaporation through membrane T4 at 15°C under the operating pressure of 400 Pa (3.0 torr): (——) calculated, according to eqs. (10) and (16), and taking the values for coefficients summarized in Table III.

membrane is given by

$$J_E = -D_{0,E} \exp(b_{EE}\bar{C}_E)\, d\bar{C}_E/dx \tag{8}$$

At the steady state, the solution of eq. (8) when the boundary conditions is

$$\bar{C}_E = \bar{C}_{E,0} \quad (= K_E C_{E,0}) \quad \text{at } x = 0$$

$$\bar{C}_E = \bar{C}_{E,x} \quad \text{at } x = x$$

is given by

$$\frac{\bar{C}_{E,x}}{\bar{C}_{E,0}} = \frac{1}{B_{EE}C_{E,0}} \ln\left[\exp(B_{EE}C_{E,0}) - \frac{B_{EE}J_E}{P_{0,E}}x\right] \tag{9}$$

Here, K_E is the solubility coefficient of ethanol. By making use of eq. (9), we are able to obtain the concentration distribution at the steady state in the membrane as shown later in Figure 8. The assumption of ethanol concentration ($\bar{C}_E$) at the downstream side of the membrane ($x = l$) being zero, which is generally regarded, leads to the derivation eq. (10) from eq. (9):

$$J_E = \frac{P_{0,E}}{B_{EE}l}\left[\exp(B_{EE}C_{E,0}) - 1\right] \tag{10}$$

Here $P_{0,E}$ ($= D_{E,0}K_E$) is the permeability coefficient at zero concentration of ethanol.

Next, we describe the water permeation through membranes T1–T4. As shown in Figure 7, water flux dependence gave a complicated profile having a maximum flux value. The fact that these membranes were swollen by ethanol, the diffusion coefficient for water is expected to depend on the local concentra-

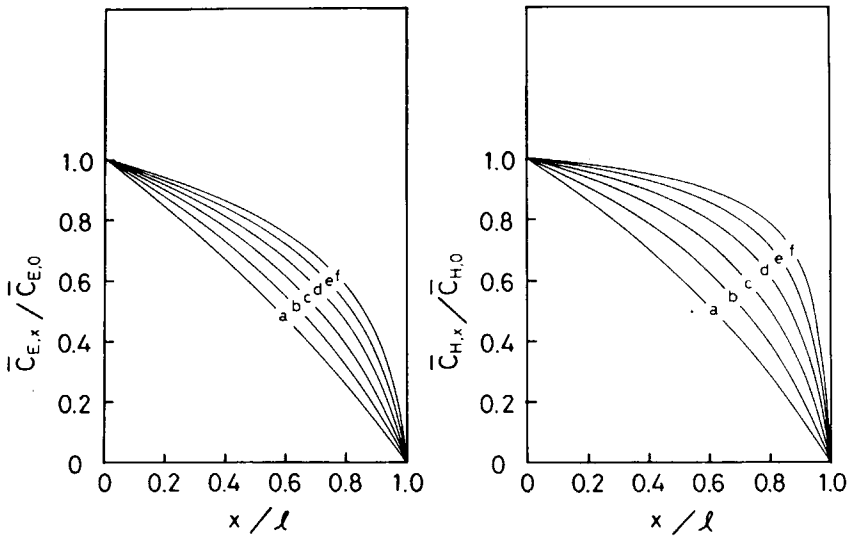

Fig. 8. Calculated concentration profiles for membrane T4 at 15°C under the operating pressure of 400 Pa (3.0 torr): (——) calculated, according to eqs. (9) and (14), and taking the values for coefficients summarized in Table III.

	a	*b*	*c*	*d*	*e*	*f*
$10^{-3}C_{E,0}$ (mol m^{-3})	2.512	5.010	7.510	10.01	12.51	15.00
$10^{-3}C_{H,0}$ (mol m^{-3})	48.02	40.79	33.27	25.30	17.01	8.421

tion of ethanol. The general expression may be given, in which the exponential depends separately on the local concentrations of ethanol and water:

$$D_H = D_{0,H} \exp(b_{HH}\bar{C}_H + b_{HE}\bar{C}_E) \tag{11}$$

However, in the present case, the diffusion coefficient of water can safely be regarded to depend on the local concentration of ethanol only as in

$$D_H = D_{0,H} \exp(b_{HE}\bar{C}_E) \tag{12}$$

Combination of eq. (12) and Fick's first law of diffusion gives water flux through the membrane:

$$J_H = -D_{0,H}(b_{HE}\bar{C}_E)\, d\bar{C}_H/dx \tag{13}$$

At the steady state, the integration of eq. (12) when the boundary conditions are

$$\bar{C}_E = \bar{C}_{E,0} \quad (= K_E C_{E,0}),$$

$$\bar{C}_H = \bar{C}_{H,0} \quad (= K_H C_{H,0}) \quad \text{at } x = 0$$

$$\bar{C}_E = \bar{C}_{E,x}, \quad \bar{C}_H = \bar{C}_{H,x} \quad \text{at } x = x$$

is given by:

(i) In the case $B_{EE} \neq B_{HE}$,

$$\frac{\bar{C}_{H,x}}{\bar{C}_{H,0}} = 1 - \frac{J_H P_{0,E}}{J_E P_{0,H}} \times \frac{\left[\exp(B_{EE}C_{E,0})\right]^{(1-B_{HE}/B_{EE})} - \left[\exp(B_{EE}C_{E,0}) - (B_{EE}J_E/P_{0,E})x\right]^{(1-B_{HE}/B_{EE})}}{(B_{EE} - B_{HE})C_{H,0}} \tag{14}$$

(ii) In the case $B_{EE} = B_{HE} = B$,

$$\frac{\bar{C}_{H,x}}{\bar{C}_{H,0}} = 1 - \frac{J_H P_{0,E}}{J_E P_{0,H}} \times \frac{BC_{E,0} - \ln\left[\exp(BC_{E,0}) - (BJ_E/P_{0,H})x\right]}{BC_{H,0}} \tag{15}$$

We can also obtain the concentration distribution in the membrane by making use of either eqs. (14) or (15) as shown in Figure 8. The assumption of both ethanol and water concentration ($\bar{C}_E$ and $\bar{C}_H$) at the downstream side of the membrane ($x = l$) being zero leads eqs. (16) and (17), respectively, from eqs. (14) and (15):

(i) In the case $B_{EE} \neq B_{HE}$,

$$J_H = \frac{P_{0,H}}{B_{EE}l}(B_{EE} - B_{HE}) \times \frac{\left[\exp(B_{EE}C_{E,0}) - 1\right]C_{H,0}}{\left[\exp(B_{EE} - B_{HE})C_{E,0}\right] - 1} \tag{16}$$

(ii) In the case $B_{EE} = B_{HE} = B$,

$$J_H = \frac{P_{0,H}C_{H,0}}{BC_{E,0}l}\left[\exp(BC_{E,0}) - 1\right] \tag{17}$$

In the present paper, water permeation was represented by eq. (16). The four parameters in the flux equations, determined to fit Figure 7 best, are summarized in Table III. Permeability coefficients in the limit of zero permeant concentration P_0 for both ethanol and water, except those of the T3 membrane, $P_{0,E}$ and $P_{0,H}$, tended to increase with the increase in 1 content in the membrane. Coefficients of the exponent model B_{EE} and B_{HE} increased with the increase in 1 fraction in the membrane. This increase of B_{EE} and B_{HE} values with the increase in 1 content is parallel to membrane swelling property with ethanol and DEM values summarized in Table II.

TABLE III
Parameters for Membranes[a]

Membrane	$10^6 l$ (m)	$10^{10} P_{0,E}$ ($m^2\ h^{-1}$)	$10^{10} P_{0,H}$ ($m^2\ h^{-1}$)	$10^4 B_{EE}$ ($m^3\ mol^{-1}$)	$10^4 B_{HE}$ ($m^3\ mol^{-1}$)
T1	8	1.6	1.1	1.9	2.9
T2	11	1.9	1.2	2.1	3.3
T3	10	4.5	2.3	2.2	3.5
T4	9	2.1	1.2	2.4	3.7

[a] Operating pressure, 400 Pa (3.0 torr); operating temperature, 15°C.

The lines for fluxes in Figures 5 and 7 are calculated ones according to eqs. (10) and (16), and taking the coefficient values summarized in Table III. Theoretical flux values under the operating pressure of 400 Pa in Figure 7 agreed well with the observed values.

As mentioned above, we can obtain the concentration distribution at the steady state in the membrane according to eqs. (9) and (14), and taking the obtained coefficients values in these two equations. As an example, ethanol and water distribution in membrane T4 under the operating pressure of 400 Pa is shown in Figure 8.

Separation Factor

Equations for separation factor may be obtained from eqs. (10), (16), and (17):

(i) In the case $B_{EE} \neq B_{HE}$,

$$\alpha = \frac{J_E/J_H}{C_{E,0}/C_{H,0}} = \frac{P_{0,E}}{P_{0,H}} \frac{\exp[(B_{EE} - B_{HE})C_{E,0}] - 1}{(B_{EE} - B_{HE})C_{E,0}} \tag{18}$$

(ii) In the case $B_{EE} = B_{HE} = B$,

$$\alpha = \frac{P_{0,E}}{P_{0,H}} \tag{19}$$

Calculated separation factors are shown in Figure 5, according to eq. (18). In Figure 5, theoretical separation factor under the operating pressure of 400 Pa gave good agreement with experimental results except that at the ethanol feed fraction of around 0.1. Disagreement of the calculated separation factor and the observed one at the ethanol fraction of around 0.1 in Figure 5 might be due to the small aliquot to be analyzed.

In Figure 9, the schematic profile of separation factor is plotted against $(B_{EE} - B_{HE})C_{E,0}$. In the present case, B_{HE} values were larger than B_{EE} ones under the operating pressure of 400 Pa. That is, the dependence of the

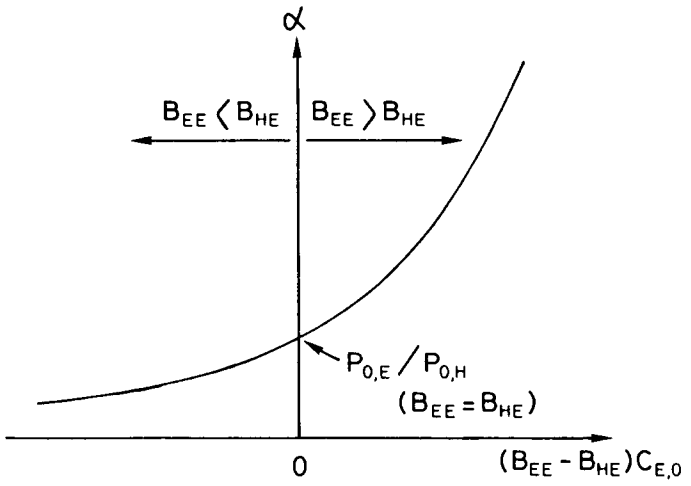

Fig. 9. Schematic dependence of separation factor on feed composition.

separation factor on the ethanol feed fraction was situated in the second quadrant. As shown in Figure 9, the separation factor increased with decrease of the ethanol feed fraction. The experimental results coincided with calculation as shown in Figure 5.

In the present paper, permeation mechanism was analyzed in terms of concentration-dependent diffusion coefficient. However, both diffusivity and solubility would depend on internal concentration of ethanol. As a further extension of this kind of study, it is necessary to represent ethanol and water fluxes by making use of equations, of which diffusion coefficients and solubility coefficients depends on internal ethanol concentration.

Thinking over the separation factor of ethanol from aqueous ethanol solution, there are a couple of ways to use membranes as mentioned in the introduction: One is to concentrate ethanol from dilute ethanol solution such as a 5–10% aqueous ethanol solution. The other one is to break the azeotropic point to obtain absolute ethanol. The present membranes have possibility to be applied to the former way.

CONCLUSION

Membranes obtained from copolymer, poly(tert-butyl methacrylate-co-styrene), which consisted of common vinyl monomers, showed selective separation of ethanol from aqueous ethanol solution. These membranes, especially gave relatively good membrane performance at the low ethanol feed concentration region. These results suggest that such common polymer membranes have potential capability to permeate ethanol preferentially from the ethanol–water mixture by the pervaporation technique. The pervaporation of the ethanol–water mixture through the present membranes was analyzed. The diffusion coefficients for both ethanol and water were exponential functions of ethanol concentration.

APPENDIX: NOMENCLATURE

b_{EE} coefficient of the exponential model for ethanol which depends on the nature of ethanol ($m^3\ mol^{-1}$)
b_{HE} coefficient of the exponential model for water which depends on the nature of ethanol ($m^3\ mol^{-1}$)
B coefficient of the exponential model for both ethanol and water ($= B_{EE} = B_{HE}$) ($m^3\ mol^{-1}$)
B_{EE} coefficient of the exponential model for ethanol ($= K_E b_{EE}$) ($m^3\ mol^{-1}$)
B_{HE} coefficient of the exponential model for water ($= K_H b_{HE}$) ($m^3\ mol^{-1}$)
$\bar{C}_E$ internal concentration of ethanol ($mol\ m^{-3}$)
$\bar{C}_H$ internal concentration of water ($mol\ m^{-3}$)
$\bar{C}_{E,0}$ internal concentration of ethanol at the upstream face of the membrane ($mol\ m^{-3}$)
$\bar{C}_{H,0}$ internal concentration of water at the upstream face of the membrane ($mol\ m^{-3}$)
$\bar{C}_{E,x}$ internal concentration of ethanol at the abscissa x ($mol\ m^{-3}$)
$\bar{C}_{H,x}$ internal concentration of water at the abscissa x ($mol\ m^{-3}$)
$\bar{C}_{E,l}$ internal concentration of ethanol at the downstream face of the membrane ($mol\ m^{-3}$)
$\bar{C}_{H,l}$ internal concentration of water at the downstream face of the membrane ($mol\ m^{-3}$)
$C_{E,0}$ concentration of ethanol in the feed solution ($mol\ m^{-3}$)
$C_{H,0}$ concentration of water in the feed solution ($mol\ m^{-3}$)
D_E diffusion coefficient of ethanol ($m^2\ h^{-1}$)
D_H diffusion coefficient of water ($m^2\ h^{-1}$)
$D_{0,E}$ diffusion coefficient at zero concentration of ethanol ($m^2\ h^{-1}$)
$D_{0,H}$ diffusion coefficient at zero concentration of water ($m^2\ h^{-1}$)
J total flux ($g\ m^{-2}\ h^{-1}$)
J_E flux of ethanol ($mol\ m^{-2}\ h^{-1}$)
J_H flux of water ($mol\ m^{-2}\ h^{-1}$)
K_E solubility coefficient of ethanol ($mol\ m^{-3}$ polymer membrane/$mol\ m^{-3}$)
K_H solubility coefficient of water ($mol\ m^{-3}$ polymer membrane/$mol\ m^{-3}$)
l thickness of the membrane (m)
$P_{0,E}$ permeability coefficient at zero concentration of ethanol ($= D_{0,E} K_E$) ($m^2\ h^{-1}$)
$P_{0,H}$ permeability coefficient at zero concentration of water ($= D_{0,H} K_H$) ($m^2\ h^{-1}$)
x abscissa across the membrane (m)

References

1. *Fermentation Ind.*, **39**, nos. 6–9 (1981) (special issue featuring article on the ethanol production).
2. S. Ueda, *Kagaku Kōgaku*, **45**, 297 (1981).
3. S. Suzuki, Ed., *Baiomasu Enerugī Henkan*, Kōdansha Scientific, Tokyo, 1983.
4. *Kagaku Kōgaku* (*Chemical Engineering*) *Symposium Series No. 14*, The Society of Chemical Engineering, Japan, 1987.
5. V. Balzani et al., *Science*, **189**, 852 (1975).
6. G. Porter and M. D. Archer, *Interdis. Sci. Rev.*, **1**, 119 (1976).
7. M. S. Wrighton, *Acc. Chem. Res.*, **12**, 303 (1979).
8. A. J. Bard, *J. Photochem.*, **10**, 59 (1979).
9. A. Heller, *Acc. Chem. Res.*, **14**, 154 (1981).
10. K. Weissermel and H. -J. Arpe, *Industrielle Organische Chemie*, 2nd ed., Verlag Chemie GmbH, Weinheim, 1976.
11. M. Yoshikawa, T. Yukoshi, K. Sanui, and N. Ogata, *J. Appl. Polym. Sci.*, **33**, 2369 (1987), and Refs. 3–14 and 25–38 therein.
12. Eustache and G. Histi, *J. Membr. Sci.*, **8**, 105 (1981).
13. K. C. Hoover and S. -T. Hwang, *J. Membr. Sci.*, **10**, 253 (1982).
14. S. Kimura and T. Nomura, *Maku* (*Membrane*), **8**, 117 (1983).
15. M. H. V. Mulder, J. O. Hendrikman, H. Hegeman, and C. A. Smolders, *J. Membr. Sci.*, **16**, 269 (1983).
16. P. Schissel and R. A. Orth, *J. Membr. Sci.*, **17**, 109 (1984).
17. K. Ishihara, Y. Nagase, and K. Matsui, *Makromol. Chem., Rapid Commun.*, **7**, 43 (1986).

18. T. Masuda, B. -Z. Tang, and T. Higashimura, *Polym. J.*, **18**, 565 (1986).
19. H. Toya, M. Ohgizawa, and H. Nishide, *Kobunshi Ronbunshu*, **43**, 559 (1986).
20. K. Ishihara, R. Kogure, and K. Matsui, *Kobunshi Ronbunshu*, **43**, 779 (1986).
21. M. Yoshikawa, T. Yukoshi, K. Sanui, and N. Ogata, *J. Polym. Sci., Polym. Chem. Ed.*, **24**, 1585 (1986).
22. H. Suematsu, K. Harada, T. Kataoka, *Maku (Membrane)*, **12**, 95 (1987).
23. S. Nakao, F. Saitoh, T. Asakura, K. Toda, and S. Kimura, *J. Membr. Sci.*, **30**, 273 (1987).
24. M. Yoshikawa, T. Yukoshi, K. Sanui, N. Ogata, and T. Shimidzu, *Maku (Membrane)*, **12**, 158 (1987).
25. M. Yoshikawa, T. Ohsawa, M. Tanigaki, and W. Eguchi, *J. Polym. Sci., Polym Lett. Ed.*, **26**, 89 (1988).
26. T. Shimidzu and M. Yoshikawa, *Polym. J.*, **15**, 135 (1983).
27. M. Yoshikawa, N. Ogata, and T. Shimidzu, *J. Membr. Sci.*, **26**, 107 (1986).
28. C. M. Hansen and B. Beerbower, *Encyclopedia of Chemical Technology*, 2nd ed., A. Standen, ed., Wiley-Interscience, New York, 1971, Suppl. Vol. A, pp. 889–910.
29. D. M. Koenhen and C. A. Smolders, *J. Appl. Polym. Sci.*, **19**, 1163 (1975).
30. T. Matsuura, *Goseimaku no Kiso*, Kitami Shobo, Tokyo, 1981, pp. 25–31.
31. C. M. Hansen and P. E. Pierce, *Ind. Eng. Chem., Prod. Res. Dev.*, **31**, 218 (1974).
32. J. A. Riddick and W. B. Bunger, *Organic Solvents*, 3rd ed., Wiley, New York, 1970.
33. F. W. Greenlaw, R. A. Shelden, and E. V. Thompson, *J. Membr. Sci.*, **2**, 333 (1977).
34. M. Yoshikawa, H. Yokoi, K. Sanui, and N. Ogata, Polym. J., **17**, 363 (1985).
35. M. Yoshikawa, T. Yukoshi, K. Sanui, and N. Ogata, *Maku (Membrane)*, **10**, 247 (1985).
36. M. Yoshikawa, Y. Adachi, K. Sanui, and N. Ogata, *Polym. J.*, **17**, 1281 (1985).
37. M. Yoshikawa, Y. Adachi, H. Yokoi, K. Sanui, and N. Ogata, *Macromolecules*, **19**, 47 (1986).
38. M. Yoshikawa, T. Yukoshi, K. Sanui, and N. Ogata, *Polym. J.*, **18**, 447 (1986).
39. G. S. Park *Trans. Faraday Soc.*, **46**, 684 (1950).
40. P. E. Rouse Jr., *J. Am. Chem. Soc.*, **69**, 1068 (1957).
41. D. W. McCall, *J. Polym. Sci.*, **26**, 151 (1957).
42. C. E. Rogers, V. Stannett, and M. Szwarc, *J. Polym. Sci.*, **45**, 61 (1960).
43. H. K. Frensdorff, *J. Polym. Sci., Part A*, **2**, 341 (1964).
44. P. Meares, *J. Appl. Polym. Sci.*, **9**, 917 (1965).
45. I. Cabasso, J. Jaguar-Grodzinski, and D. Vofsi, *J. Appl. Polym. Sci.*, **18**, 2117 (1974).
46. I. Cabasso, *Ind. Eng. Chem., Prod. Res. Dev.*, **22**, 313 (1983).

Received August 7, 1987
Accepted November 20, 1987